



DETERMINATION OF DIFFUSION COEFFICIENT OF  
TRANSPARENT SOLUTIONS USING  
MOIRE'DEFLECTOMETRY

By

Getachew Alemu

SUBMITTED IN PARTIAL FULFILLMENT OF THE  
REQUIREMENTS FOR THE DEGREE OF  
MASTER OF SCIENCE

AT

ADDIS ABABA UNIVERSITY

ADDIS ABABA, ETHIOPIA

JULY 2007

ADDIS ABABA UNIVERSITY  
DEPARTMENT OF  
PHYSICS

The undersigned hereby certify that they have read and recommend to the Faculty of Science for acceptance a thesis entitled **“Determination Of Diffusion Coefficient of transparent Solutions Using Moire’Defelectometry”** by **Getachew Alemu** in partial fulfillment of the requirements for the degree of **Master of Science**.

Dated: July 2007

Supervisors:

\_\_\_\_\_  
Prof. A.V.Gholap

Examiner:

\_\_\_\_\_  
  
\_\_\_\_\_

ADDIS ABABA UNIVERSITY

Date: **July 2007**

Author: **Getachew Alemu**

Title: **Determination Of Diffusion Coefficient of  
transparent Solutions Using  
Moire'Deflectometry**

Department: **Physics**

Degree: **M.Sc.** Convocation: **July** Year: **2007**

Permission is herewith granted to Addis Ababa University to circulate and to have copied for non-commercial purposes, at its discretion, the above title upon the request of individuals or institutions.

---

Signature of Author

THE AUTHOR RESERVES OTHER PUBLICATION RIGHTS, AND NEITHER THE THESIS NOR EXTENSIVE EXTRACTS FROM IT MAY BE PRINTED OR OTHERWISE REPRODUCED WITHOUT THE AUTHOR'S WRITTEN PERMISSION.

THE AUTHOR ATTESTS THAT PERMISSION HAS BEEN OBTAINED FOR THE USE OF ANY COPYRIGHTED MATERIAL APPEARING IN THIS THESIS (OTHER THAN BRIEF EXCERPTS REQUIRING ONLY PROPER ACKNOWLEDGEMENT IN SCHOLARLY WRITING) AND THAT ALL SUCH USE IS CLEARLY ACKNOWLEDGED.

*TO WORDS OF GOD*

*.For I know the plan that I have for you*

# Table of Contents

<b>Table of Contents</b>	<b>v</b>
<b>List of Tables</b>	<b>vii</b>
<b>List of Figures</b>	<b>viii</b>
<b>Abstract</b>	<b>x</b>
<b>Acknowledgement</b>	<b>xi</b>
0.1 Introduction . . . . .	1
0.2 Objectives . . . . .	3
0.2.1 General Objectives . . . . .	3
0.2.2 Specific Objectives . . . . .	3
<b>1 DIFFUSION AND DIFFUSION EQUATION</b>	<b>6</b>
1.1 Basic hypothesis of Mathematical theory . . . . .	6
1.2 The Diffusion Process . . . . .	7
1.3 The Empirical laws of Diffusion . . . . .	9
1.4 Diffusion Coefficient and Mean free Path . . . . .	11
1.5 Diffusion Coefficient and Viscosity . . . . .	13
1.6 Random Walk as a statical Model for Diffusion . . . . .	14
<b>2 Moire'and Moire'Defelectometry</b>	<b>17</b>
2.1 Interfrenec Fringes on Screen . . . . .	17
2.2 Theory of Interference . . . . .	17
2.3 Diffraction . . . . .	20
2.3.1 The Plane Diffraction Grating . . . . .	21
2.4 Moire'and Fringe Projection Techniques . . . . .	21
2.4.1 What is Moire' . . . . .	22

2.4.2	Fringe Projection Techniques . . . . .	28
2.4.3	Shadow Moire' . . . . .	30
2.4.4	Projection Moire' . . . . .	34
2.5	Moire Defeectometry . . . . .	35
2.5.1	Phase Measuring Defeectometry . . . . .	40
2.6	Diffusion Coefficient and Moire'Fringe Shift. . . . .	42
<b>3</b>	<b>Experimental Technique</b>	<b>48</b>
3.1	Materials and Methods of the Experiment . . . . .	48
3.2	Experimental Methods and Procedures . . . . .	48
3.3	Procedure . . . . .	49
3.4	Materials Used . . . . .	50
<b>4</b>	<b>Results, Analysis and Discussion</b>	<b>51</b>
4.1	Determination of diffusion coefficient of Sugar Solution in different concentration . . . . .	51
4.1.1	Sugar Solution Concentration 2.5 percent . . . . .	51
4.1.2	Sugar solution concentration 5 percent . . . . .	52
4.1.3	Sugar Solution Concentration 7.5 percent . . . . .	54
4.1.4	Sugar Solution Concentration 10 percent . . . . .	54
4.1.5	Sugar Solution Concentration 12.5 percent . . . . .	56
4.1.6	Sugar Solution Concentration 15 percent . . . . .	57
4.1.7	Sugar Solution Concentration 17.5 percent . . . . .	59
4.1.8	Sugar Solution Concentration 20 percent . . . . .	59
4.1.9	Discussion . . . . .	61
4.1.10	Diffusion Vs concentration graph . . . . .	63
<b>5</b>	<b>Conclusion</b>	<b>64</b>
5.1	Conclusion . . . . .	64
	<b>Bibliography</b>	<b>66</b>

# List of Tables

# List of Figures

1.1	The motions of molecules or atoms appear to be random walk. . . . .	8
1.2	Diffusion and random motion. . . . .	16
2.1	Interference of monochromatic light . . . . .	18
2.2	Moire'fringes at small angle tilt. . . . .	22
2.3	Moire'between two straight-line gratings of the same pitch at angle $2\alpha$ with respect to each other. . . . .	23
2.4	Moire pattern caused by two straight-line gratings with (a)the same pitch tilted with respect to one another, (b)different frequencies and no tilt,and (c) different frequencies tilted with respect to one another.	26
2.5	Geometry used to determine spacing and angle between two gratings of different frequencies . . . . .	27
2.6	Projection of fringes or gratings onto an object and observing it at angle $\alpha$ . P is gratings(pitch) and C the contour interval. . . . .	29
2.7	Maximum sensitivity for fringe projection at $90^\circ$ . . . . .	30
2.8	Fringe produced by two interfering beams . . . . .	31
2.9	Geometry for shadow moire' where illumination and viewing points are at infinity. . . . .	32
2.10	Shadow moire when both illumination and viewing positions are at finite distances. . . . .	33
2.11	Projection Moire fringe . . . . .	35
2.12	Experimental arrangement of laser moire defelectometry. . . . .	37

2.13	Spatial frequency distribution of moire' fringes . . . . .	42
3.1	Experimental set up . . . . .	49
4.1	Fringe Shift in 2.5 percent sugar solution . . . . .	52
4.2	Fringe Shift in 5 percent sugar solution . . . . .	53
4.3	Fringe Shift in 7.5 percent sugar solution . . . . .	55
4.4	Fringe Shift in 10 percent sugar solution . . . . .	56
4.5	Fringe Shift in 12.5 percent sugar solution . . . . .	57
4.6	Fringe Shift in 15 percent sugar solution . . . . .	58
4.7	Fringe Shift in 17.5 percent sugar solution . . . . .	60
4.8	Fringe Shift in 20 percent sugar solution . . . . .	61
4.9	Diffusion Coefficient Vs Concentration . . . . .	63

# Abstract

In this thesis the Moire' Deflectometry technique is applied to the investigation of diffusion dynamics in transparent liquid mixtures. It describes the theoretical analysis for obtaining the magnitude of diffusion coefficient using moire' fringe patterns. The theoretical aspects of the methods presented show the relationship between the moire' fringe shift and diffusion coefficient. Based on the moire' effect, the displacement (moire' fringe shift position) can be used to calculate the deflection angle of a laser beam, which is induced by the variation of refractive index. The physical and mathematical model of laser moire' deflectometry is presented in detail.

In the diffusion of a high concentration sugar solution, the formation of a dense layer above the initial boundary of two liquids was observed. This may be related to so-called baro-diffusion effect - the influence of gravity on diffusing molecules, that forms the upward motion of sugar molecules, which is balanced by gravity.

**Key Words :** Moire' Deflectometry, Fringe Projection, Moire' Fringes, Grating, Moire' Fringes, Index of Refraction, Moire' fringe shift.

# Acknowledgement

First and foremost,I thank God for everything was possible in his will.I wish to express my sincere gratitude to my advisor Professor A.V Gholap for his initiation,his continues follow up, motivation, and his smooth but efficient communication throughout the research.

I would like to thank Dr.Tialun Tesfaye for the provision of digital camera. I am also grateful to My Famlies, Admasu Tassew,Abiy Dejene,Getachew Worku, Kusse Gudish and Sisay Mebre.

Getachew Alemu

July, 2007

## 0.1 Introduction

Diffusion can be the random walk of an ensemble of particles from the region of higher concentration to region of lower concentration [1, 16]. The process plays an important role in many fields of the study in physics, chemistry, Mechanical Engineering etc. It helps the study of crystal growth, pollution control, separation of isotopes, doping of impurities and also to study some biological systems. Interference optical methods of observing the refractive index gradient change occurring in an initially sharp diffusing boundary has been developed to study diffusion coefficient of different kind of solution or fluids by Coulson, Cox, Ogston and Philopt (1948), and Ogston (1949). They developed an apparatus called Gouy Diffusimeter. It mainly served for measuring rapidly diffusing substances such as protein [5, 10].

Laser based techniques are among the most sensitive methods employed for measuring diffusion coefficient and thermal Conductivity. Their advantages are that they are non-contact methods that allow remote monitoring; show less sensitivity to vibration, have very high spatial precision, fast response time and reliable. This is possible through the development and application of moire' fringe projection and moire' deflectometry. Lord Rayleigh noticed the phenomena of moire fringe in 1874. He used to look at the moire' between two identical gratings to determine their quality. Righi (1887), first showed the relative displacement of two gratings could be determined by observing the movement of the moire fringes [2, 3].

Wave front compression methods such as optical and holographic interferometry are among the widely used techniques for diffusive studies. But the limitation of these techniques are their sensitivity to variations. Also the data has to be processed manually to obtain derivatives of the phase shift.

The next significance in the use of moiré was presented by Weller and Shepherd (1948). They used moiré to measure the deformation of an object under applied stress by looking at the difference in grating pattern before and after applied stress. They were the first to use shadow moiré where a grating is placed in front of non-flat surface to determine the shape of the object behind it by using the shape of moiré fringe. A rigorous theory of moiré fringe did not exist until the mid fifties when Ligtenberg (1955) and Guild (1956, 1960) explained moiré for stress analysis by mapping slope contour and displacement measurement, respectively. In (1967) Rowel and Wolford used fringe projection technique to determine surface topography. The technique entails projecting a fringe or grating on an object and viewing it from different directions [11, 25].

The technique was used by Brooks and Helifinger (1969) for optical gauging and deformation measurement. Until 1970, advances in moiré techniques were primarily in stress analysis. Some of the first uses of moiré to measure surface topography were reported by Meadow et al (1970), Takasaki (1970), and Wasowski (1970) [4, 7].

A theoretical review and experimental comparison of moiré and projection technique for contouring is given by Benoit et al. (1975). Automatic computer fringe analysis for moiré pattern by finding fringe centers were reported by Ytagai et al. (1982). Among these techniques the moiré deflectometry is vital for the study of diffusivity of miscible fluids flow. The molecular diffusion coefficient of fluid can be determined using physical relation between changes in the optical path length and phase properties as a function of time and concentration at a constant temperature. The technique is applied to measuring the diffusion coefficient of transparent liquid solution of sugar in pure water [25].

Moire fringe projection and moire' defelectometry are among the active areas of study in recent time. Among these areas are: Ray deflection approach to optical testing for diagnosis of phase of phase object and specular surface of optical devices, the measurement of modulation transfer function of Electro-Optical system and their compensates such as X-ray imaging intensifier tube and florescence screen, visualizing flow field in a diesel combustion chamber and determination of temperature distribution of its flow field qualitatively, turbulent flow of gas and temperature distribution of flame, and the moire' defelectometric technique for measuring the diffusion coefficient of transparent solution which was introduced in 2004 by group of researchers Kazem Jamshide-Ghaleh, Mohammed Taghi Tavassoly and Nastaran Mansour [11, 20].

## **0.2 Objectives**

### **0.2.1 General Objectives**

The main objectives of this thesis are

- (i). to determine the diffusion coefficient of transparent liquid solution (e.g. sugar solution at different concentration) in pure water using Laser moire' defelectometry.
- (ii). the economical utility of technique.
- (iii). an appropriate design of apparatus from locally available materials.

### **0.2.2 Specific Objectives**

The specific objectives of the experiment are to measure the diffusion coefficient of sugar at different concentration and time at constant temperature. The moire fringe shifts due to ray deflection. This shift is measured for the different concentrations and analysis is done to determine the diffusion coefficient of their solution in distilled

water.



# Chapter 1

## DIFFUSION AND DIFFUSION EQUATION

### 1.1 Basic hypothesis of Mathematical theory

Transfer of heat by conduction like diffusion is a random process in which from one part to another by random molecular motions and there is an obvious analogy between the two processes. This was recognized by Fick's (1855), who first put diffusion on a quantitative basis by adopting the mathematical equation of heat conduction derived some years earlier by Fourier (1822). The mathematical theory of diffusion in isotropic substances is therefore based on the hypothesis that the rate of transfer of diffusing substance through unit area of a section is proportional to the concentration gradient measured normal to the section.[1, 4]

$$F = -D \frac{\partial C}{\partial X} \quad (1.1.1)$$

-Ve sign arises because diffusion occurs in the direction opposite to that of concentration. Where: F - the rate of transfer per unit area of section, C- the concentration of diffusing substance, X - the space coordinate measured normal to the section, D- the diffusion coefficient.

In some cases e.g. Diffusion in dilute solution ( $D$ ) can reasonably be taken as a constant, while in other diffusion in high polymers, it depends very markedly on Concentration. If  $F$  the amount of material diffusing and  $C$  the concentration are both expressed in terms of the same unit of quantity, gram/gram molecules, that  $D$  is independent of this unit and has dimensions  $(Length)^2(time)^{-1}$

## 1.2 The Diffusion Process

Diffusion is the process by which matter is transported from one part of a system to another because of random molecular motions. It is usually illustrated by the classical experiment in which a tall cylindrical vessel has its lower part filled with iodine solution. For example a column of clear water is poured on top carefully and slowly, so that no convection currents are set up. At first the colored part is separated from the clear by a sharp well-defined boundary. Later it is found that the upper part becomes colored, the colors getting fainter toward the top, while the lower part becomes correspondingly less intensely colored. After sufficient time the whole solution appears uniformly colored. There is evidently therefore a transfer of iodine molecules from the lower to the upper part of the vessel taking place in the absence of convection currents. The iodine is said to have diffused into the water.[1, 4]

If it were possible to watch individual molecules of iodine and this can be done effectively by replacing them by particles small enough to share the molecular motion but just large enough to be visible under the microscope, it would be found that the motion of each molecule is the random one. In a dilute solution each molecule of iodine behaves independently of others, which it seldom meets and each is constantly undergoing collision with solvent molecules as a result of which collisions it moves

some times to ward a region of higher, sometimes of lower, concentration, having no preferred direction of motion towards one/or the other. The motion of a single molecule can be described in terms of the familiar "random walk" picture, as shown below in fig 1.1.

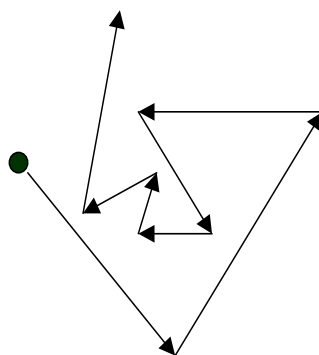


Figure 1.1: The motions of molecules or atoms appear to be random walk.

This picture of random molecular motions, in which no molecule has a preferred direction of motion, has to be reconciled with the fact that a transfer of iodine molecules from the region of higher to that of the lower concentration is never the less observed. Consider any horizontal section in the solution and two thin, equal, elements of volume one just below and one just above the section. Though it is not possible to say which way any particular iodine molecule will move in a given interval of time, it can be said that on an average a definite fraction of molecules in the lower element of volume will cross the section from below and a fraction of molecules in the upper element will cross the section from above in a given time. This occurs simply because there are more iodine molecules in the lower element than in the upper one, there is

a net transfer from the lower to the upper side of the section as a result of random molecular motions.

### 1.3 The Empirical laws of Diffusion

The phenomenological description of diffusion is embodied in Fick's two laws, which are empirical statements that relate the diffusive flow of matter to concentration gradients. To illustrate these laws, consider a single-phase dilute binary alloy in which the constituents are inhomogeneously distributed and let  $C$  be the concentration of the minor constituent. The concentration is function of position and time and the concentration gradient induces a flow of matter.[1, 16]

**Fick's First law :** "States that the flux of the diffusing species in a given direction has a magnitude proportional to the concentration gradient in that direction". That is if  $J_1$  the flux along the  $X_1$  axis, then

$$J_1 = -D_1 \frac{\partial C}{\partial X_1} \quad (1.3.1)$$

Where:  $D_1$ - proportionality factor called diffusion coefficient. The negative sign expresses the fact that diffusion occurs from the region of high concentration to region of low concentration.[10]

If  $X_1, X_2, X_3$  are the points in a Cartesian coordinate system with unit vectors  $(i_1, i_2, i_3)$  then we would expect that an equation similar to (Eq.1.3.1) hold for each of the three directions along the coordinate axis. For isotropic systems such as gases and liquids, this turns out to be the case. Further more for such systems the diffusing coefficient is experimentally found to be the same in all directions. In nonhomogeneous systems, however it is not the same in all directions. Also the flux in a one

direction can depend on the flux in other directions.[2, 17]

These results can be described by a generalized Fick's first law, as

$$J_1 = D_{11} \frac{\partial C}{\partial X_1} - D_{12} \frac{\partial C}{\partial X_2} - D_{13} \frac{\partial C}{\partial X_3} \quad (1.3.2)$$

Similarly the fluxes in other two directions of the Cartesian coordinate system are given by

$$J_2 = D_{21} \frac{\partial C}{\partial X_1} - D_{22} \frac{\partial C}{\partial X_2} - D_{23} \frac{\partial C}{\partial X_3} \quad (1.3.3)$$

$$J_3 = D_{31} \frac{\partial C}{\partial X_1} - D_{32} \frac{\partial C}{\partial X_2} - D_{33} \frac{\partial C}{\partial X_3} \quad (1.3.4)$$

These equations can be written in a compact form by defining the flu vector  $J$  as

$$J = J_1 i_1 + J_2 i_2 + J_3 i_3 \quad (1.3.5)$$

and the diffusion dyadic  $D$  as

$$D = D_{11} i_1 i_1 + D_{12} i_1 i_2 + D_{13} i_1 i_3 + D_{21} i_2 i_1 + D_{22} i_2 i_2 + D_{23} i_2 i_3 + D_{31} i_3 i_1 + D_{32} i_3 i_2 + D_{33} i_3 i_3 \quad (1.3.6)$$

The equation ref.1.3.2-1.3.5 give the generalized

Fick's First law as

$$J = -D \nabla C \quad (1.3.7)$$

**Fick's Second law** "states that the time rate of change of concentration in volume element of membrane with in the differential filed is proportional to the rate of change of flux gradient at that point in the filed" i.e

$$\frac{\partial C}{\partial t} + \nabla \cdot J = 0 \quad (1.3.8)$$

This is just an expression of law of conservation of matter and states that any change in concentration in a volume element is the result of the difference in matter flow in and out of the volume element.[10, 16].

Combining Equations 1.3.7 and 1.3.8 gives a generalized form of Fick's second law:

$$\frac{\partial C}{\partial t} = \nabla D \cdot \nabla C \quad (1.3.9)$$

In isotropic and cubic systems this takes a particularly simple form since  $D_1 = D_2 = D_3 = D$ . [9, 24] If  $D$  is a constant independent of position and time the simplification is even greater and Fick's laws become.

$$\frac{\partial C}{\partial t} = \nabla^2 C \quad (1.3.10)$$

## 1.4 Diffusion Coefficient and Mean free Path

The average distance an atom or a molecule travels between collisions is called its mean free path. The mean free path depends upon the size of the atom or molecule. For typically small molecule in the gas phase at 300K, the mean free path is about 8mm. Taking an average speed of 400m/s the average time collisions is about  $2 \times 10^{-10} \frac{m^2}{se}$ , this means this small molecules makes  $5 \times 10^9$  collisions per second.

As the molecules undergo this seemingly random motion induced by collisions with other atoms or molecules they migrate through the solution. If there are initially larger proportions of molecules of particular type in one region of the solution then over the time the molecules will spread out and become evenly distributed throughout the solution. This in the process of diffusion for an initial concentration gradient of a gas or liquid media the rate at which the molecules spread out is proportional to

the difference in the concentration gradient.[1, 24]

$$DiffusionRate = D \times Concentrationgradient \quad (1.4.1)$$

Where: $D$ -is diffusion coefficient gradient in  $\frac{(Length)^2}{Time}$ . It is a measure of the number of molecules moving through a particular cross-sectional area per unit of time. Experimental measurement of typical diffusion coefficient in water at 300K yields values in the range of  $10^{-6}cm^2/s$ .

Diffusion coefficient is related to the mean free path that a molecule travels via Einstein-Smoluchowsky equation.

$$D = \frac{\lambda^2}{2\tau} \quad (1.4.2)$$

where: $\lambda$  - is the mean free path,  $\tau$ - average time between collisions. Assuming that the average time between the collisions can be calculated from the average speed and mean free path, the time between the collisions can be expressed as

$$\tau = \frac{\lambda}{V_{av}} \quad (1.4.3)$$

Where: $V_{av}$  is the average speed of molecule.

Combining Equ. 1.4.2 and 1.4.3 gives

$$D = \frac{\lambda V_{av}}{2} \quad (1.4.4)$$

Using the gas phase value of 80nm for the mean free path and 400m/s as the average speed the predicated diffusion coefficient for a small molecule is  $1.6 \times 10^{-6}m^2/s$ , which is much larger than the typical value for the diffusion coefficient of liquid phase  $10^{-9}m^2$  [8, 13]

## 1.5 Diffusion Coefficient and Viscosity

The transport property which is most important for the fluid to flow is the viscosity. Viscous forces appear only when adjacent part of fluid is moving with different velocities. Thus in the flow of liquid down a pipe the liquid layer which is usually in contact with the pipe is stationary and the axial region is moving with maximum velocity. Common experience is that high viscosity liquid will flow more slowly than a low viscosity liquid, like water for a given applied pressure difference.

Poiseuille's formula for the flow of liquid in a capillary of radius  $R$  and length  $l$  is

$$\frac{dV}{dt} = \frac{(P_1^2 - P_2^2)\pi R^4}{16\lambda\eta P} \quad (1.5.1)$$

where:  $V$  is the volume of flowing,  $P_1$  and  $P_2$ , are the pressure at each end of the tube,  $P$  is the pressure at which the when Volume is measured and  $\eta$  is the coefficient of viscosity. [13] Diffusion in the fluid medium is related to a measurable property called viscosity. Viscosity is the measure of the resistance to the fluid flow. Liquid such as water that flow easily have a relatively low viscosity compared to thicker fluids.

The viscosity of liquid is also its measure to transport momentum. Its unit is poise  $P$  where  $1P = 0.1 \frac{Kg}{m.s}$ . Typical viscosities are in the range of  $10^{-4}P$  for gas and  $10^{-2}P$  for liquids. For a gas kinetic theory predict that viscosity is independent of pressure and proportional to the square root of the absolute temperature. For liquid viscosities have an exponential dependence on the temperature as described by the formula

$$\eta = A \exp\left[\frac{\Delta E_V}{RT}\right] \quad (1.5.2)$$

Where:  $\Delta E_V$ -an activation barrier.  $R$ -is the radius of the molecule.  $T$ -is the temperature. The relation between diffusion coefficient and viscosity is given by Einstein Stokes equation

$$D = \frac{KT}{6\pi\eta R} \quad (1.5.3)$$

Where:  $K$ -is Boltzman's constant.  $T$ -temperature.  $R$ -is the radius of the molecule. The equation is derived, of course, assuming that the molecule is spherical in shape. The Einstein-Stokes equation that the viscosity and diffusion coefficient are inversely related to  $D_0$  is also related to temperature via the equation.[13, 24]

$$D = D_0 \exp\left[\frac{-E_A}{RT}\right] \quad (1.5.4)$$

Where:  $D_0$ -is the diffusion coefficient at infinite temperature (maximum diffusion coefficient).  $E_A$ -is activation energy

## 1.6 Random Walk as a statical Model for Diffusion

### One-Dimensional Treatment

Process such as diffusion in which a single molecule moves through a solution a huge number of particles, can be modeled statically. Even though the presence of other particles can affect the dynamics of the particle of interest through collision and interactions we can consider the motion of particle as a random walk. The diffusion as a motion of random walk simulation can be shown by calculating the average square distance from the origin. To do this, many individual walks simulation is carried out, and the average is taken over many individual walks.

Let us consider a distribution where the concentration depends on only one coordinate, be the x-coordinate (one - dimensional diffusion). The concentration of the

marked (atom) particle is then a function of  $X$  and of time  $t$ . Let it be  $C(X,t)$ , in order to calculate, the diffusion flow we need to count the number of particles which pass through a surface of unit area, perpendicular to the axis, in the plane  $X_0$  during time  $t$  [21].

The particles migrate through the lattice by making a sequence of jumps owing to the presence of defects. We have chosen the case of tracer-diffusion with no external applied force, so that the probability of displacement is the same along both positive and negative direction will be called  $X$ . Let us define the distribution function  $f(X, t)dt$  as the probability of displacement with a projection between  $X$  and  $X+dX$ . It follows from this definition that

$$\int_{-\infty}^{\infty} f(x, t)dx = 1 \quad (1.6.1)$$

More over since the jumps along both  $+X$  and  $-X$  direction occur with the same probability one has

$$f(X, t) = f(-X, t) \quad (1.6.2)$$

Considering a large number of particles the projection of the mean displacement  $\langle X \rangle$  may then be written as [16, 17]

$$\langle X \rangle = \int_{-\infty}^{\infty} X f(x, t)dx \quad (1.6.3)$$

It follows from Eqn.1.6.2 and every  $\langle X^{2n+1} \rangle$  is zero. The most important parameter in diffusion is the mean square displacement,  $\langle X^2 \rangle$  the projection of which is then

$$\langle X^2 \rangle = \int_{-\infty}^{\infty} X^2 f(x, t)dx \quad (1.6.4)$$

Results for  $\langle X^2 \rangle$  versus time for a random walk of one dimension is shown in fig 1.2 below.

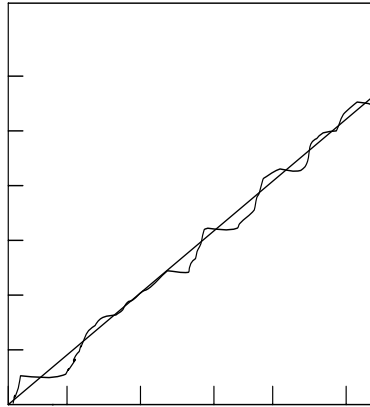


Figure 1.2: Diffusion and random motion.

The result presented on the figure shows that the system follows equation

$$\langle x^2 \rangle \propto D \cdot t \quad (1.6.5)$$

Where:  $t$  - is the time  $t$  (proportional to the number of steps)

$D$  - is the diffusion coefficient.

# Chapter 2

## Moire'and Moire'Deflectometry

### 2.1 Interference Fringes on Screen

It is a matter of common experience that two trains of ripple on the surface of water cross each other and proceed onward in their direction undisturbed. In the same way two beams of light cross each other and proceed without being influenced by each other in any way. However in the region of crossing where both beams are acting simultaneously, we expect modification in their intensity which should be either less or greater than that which would be given by one beam alone. This modification of intensity due to superposition of two or more beams of light is *interference of light* [18]

### 2.2 Theory of Interference

We shall now derive an expression for the resultant intensity at any point P on the screen due to superposition of two waves of light having equal amplitude, equal wavelength and equal velocity but initially starting with constant phase difference [9, 18]. illuminate slits  $S_1$  and  $S_2$  with monochromatic light of wavelength  $\lambda$ . The slits to be equidistant from  $S_1$  and  $S_2$ , the other slits. As a consequence waves of light

from S always arrive at  $S_1$  and  $S_2$  is equal phase and at any instant 't'. We may there represent by the equation

$$Y = a \sin 2\pi \frac{t}{T} \quad (2.2.1)$$

a-amplitude, T- period of simple parodic vibration.

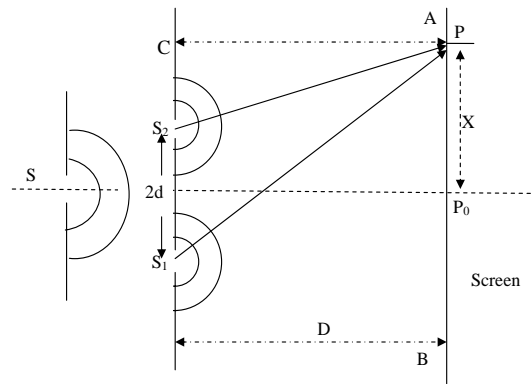


Figure 2.1: Interference of monochromatic light

In travelling from  $S_1$  to P the phase of wave alter by  $2\pi \frac{S_1P}{\lambda}$ . Hence at the instant 't', the liner displacement at P due to this wave will be expressed by

$$Y_1 = a \sin 2\pi \left( \frac{t}{T} - \frac{S_1P}{\lambda} \right) \quad (2.2.2)$$

Similarly at the instant 't' the displacement of P due to vibration of light from  $S_2$  will be represented by

$$Y_2 = a \sin 2\pi \left( \frac{t}{T} - \frac{S_2P}{\lambda} \right) \quad (2.2.3)$$

According to the principle of superposition of wave motion, the resultant displacement is given by

$$Y = Y_1 + Y_2 \quad (2.2.4)$$

$$Y = a \sin 2\pi\left(\frac{t}{T} - \frac{S_1P}{\lambda}\right) + a \sin 2\pi\left(\frac{t}{T} - \frac{S_2P}{\lambda}\right) \quad (2.2.5)$$

Let  $S_1P = \alpha$  and  $S_2P = \Delta + \alpha$  where  $\Delta = S_2P - S_1P$  is called the optical path difference between the two superposed waves at P we may now write,

$$Y = a \sin 2\pi\left(\frac{t}{T} - \frac{\alpha}{\lambda}\right) + a \sin 2\pi\left(\frac{t}{T} - \frac{\alpha + \Delta}{\lambda}\right) \quad (2.2.6)$$

$$Y = 2a \cos \frac{\Delta\pi}{\lambda} \sin\left(\frac{t}{T} - \frac{\alpha + \frac{\Delta}{2}}{\lambda}\right) \quad (2.2.7)$$

a wave of the same wave length and period as the component of waves but with amplitude

$$R = 2a \cos \pi \frac{\Delta}{\lambda} \quad (2.2.8)$$

which varies between 0 and 2a with proper variation in the magnitude of  $\Delta$ . Also if  $\delta$  is the phase difference corresponding to the path difference  $\Delta$  between the two superposed waves at p then

$$\delta = 2\pi \frac{\Delta}{\lambda} = 2\pi \frac{\Delta}{\lambda} (S_2P - S_1P) \quad (2.2.9)$$

The resultant amplitude R can now be expressed in the form

$$R = 2a \cos \frac{\pi\Delta}{\lambda} = 2a \cos \frac{1}{2} \left( \frac{2\pi\Delta}{\lambda} \right) = 2a \cos \left( \frac{\delta}{2} \right) \quad (2.2.10)$$

The resultant intensity I at point P is proportional to the square of the amplitude R, hence we write I proportional to  $4a^2 \cos^2 \frac{\delta}{2}$  which assuming the constant of proportionality to be unity for (simplicity) can be easily expressed as

$$I = 2a^2(1 + \cos \delta) \quad (2.2.11)$$

which varies with the magnitude of  $\delta$

In order to plot the intensity distribution in the interference pattern arising from the interference of light waves from two coherent sources  $S_1$  and  $S_2$  it is essential to investigate the spacing of these fringes on the screen placed parallel to the line joining  $S_1$  and  $S_2$ . At any point P on the screen the resultant intensity is maximum or minimum according as its distance from two coherent sources  $S_1$  and  $S_2$  which always in equal phase difference exactly by even or odd multiple of  $\frac{\lambda}{2}$  where  $\lambda$  the wave length of the light emitted by the sources [12, 18]. In symbols the conditions are expressed as

$$S_2P - S_1P = 2n\frac{\lambda}{2}(\text{BrightFringes}) \quad (2.2.12)$$

$$S_2P - S_1P = (2n + 1)\frac{\lambda}{2}(\text{DarkFringes}) \quad (2.2.13)$$

## 2.3 Diffraction

According to geometrical optics, if an opaque object is placed between a point light source and screen, the edges of the object will cast a sharp shadow on the screen (the penumbra will be negligible) if the sources is sufficiently, small no light will reach the screen at points with on the geometrical shadow, while out side the shadow the screen will be uniformly illuminated. A small amount of light has "bent" around the edges into the geometrical shadow which is broadened by alternate bright and dark bands. In the first bright band out side the geometrical shadow, the illumination is actually greater than in the region of uniform illumination at the extreme left .

The term diffraction applied to problems such as this one is concerned with the resultant effect produced by a limited portion of a wave front. Since in most diffraction

problems some light is found within the region of geometrical shadow, diffraction is sometimes defined as the bending of light around an obstacle[14, 18].

### 2.3.1 The Plane Diffraction Grating

An arrangement consisting of a large number of slits of the same width and separated by equal opaque spaces is known as *diffraction grating*. This was first constructed by Joseph Fraunhofer and it was due to this study of diffraction of parallel beams of light by grating in 1819 that his name became associated with this class of diffraction phenomena. The diffraction pattern suffers a modification as the number of slits is increased beyond two[5, 9].

## 2.4 Moiré and Fringe Projection Techniques

The term moiré is a French word, which refers to "an irregular wavy finish usually produced on a fabric by pressing between engraved rollers" (Webster's 1981). In optics it refers to a pattern produced between two gratings of approximately equal spacing. It can be seen in everyday things such as the overlapping of two window screens, the recreating of half-tone pictures, or with striped shirts seen on television. The use of moiré for sensitive testing was introduced by Lord Rayleigh in 1874. He looked at the moiré between two identical gratings to determine their quality even though each individual grating could not be resolved under a microscope[7, 16, 20].

Fringe projection entails projecting a fringe pattern or grating on an object and viewing it from a different direction. The first use of fringe projection for determining surface topography was presented by Row and Welford in 1967. It is convenient

technique for contouring objects that are too coarse to be measured with standard interferometry. Fringe projection is related to optical triangulation using a single point of light and light sectioning where a single line is projected onto an object and viewed in different direction to determine the surface contour (Case et al. 1987).

Moire' fringe projection interferometry complement conventional holographic interferometry, especially for testing optics to be used at long wave-lengths. Although two-wave length holography (TWH) can be used to contour surface at any longer-than-visible wavelength, visible interferometric environmental conditions are required.

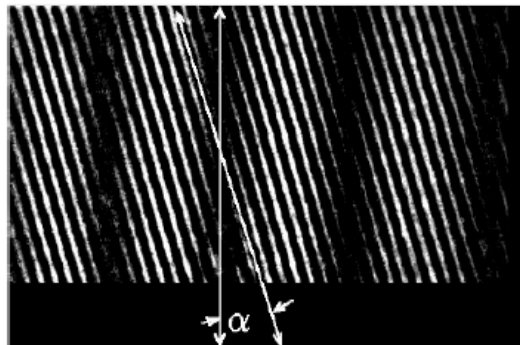


Figure 2.2: Moire' fringes at small angle tilt.

### 2.4.1 What is Moire'

Moire' patterns are extremely useful to understand basic interferometry and interferometric test results. The moire' pattern (or beat pattern) produced by two identical straight-line gratings rotated by a small angle relative to each other. A dark fringe is produced when the dark lines are out of step one-half period, and a bright

fringe is produced when dark lines for one grating fall on top of the corresponding dark lines for the second grating. If the angle between the two gratings is increased, the separation between the bright and dark fringes decreases. [A simple explanation of moiré is given by Oster and Nishijima (1963)] [4, 7, 11].

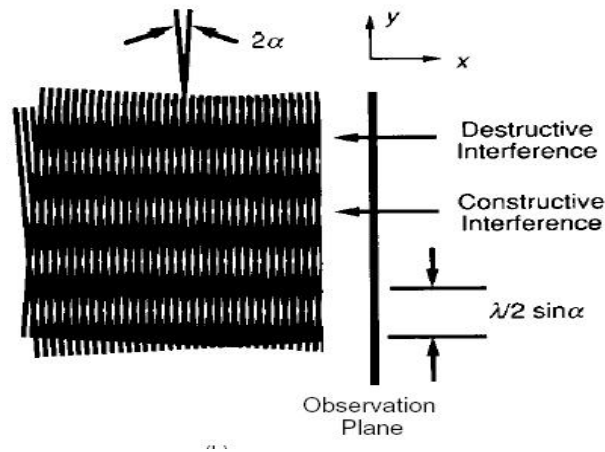


Figure 2.3: Moiré between two straight-line gratings of the same pitch at angle  $2\alpha$  with respect to each other.

The following analysis shows how to calculate the moiré pattern for arbitrary gratings .

Let the intensity transmission function for two gratings  $f_1(x, y)$  and  $f_2(x, y)$  be given by

$$f_1(x, y) = a_1 + \sum_{n=1}^{\infty} b_{1n} \cos[n\Phi_1(x, y)] \quad (2.4.1)$$

$$f_2(x, y) = a_2 + \sum_{m=1}^{\infty} b_{2m} \cos[m\Phi_2(x, y)] \quad (2.4.2)$$

Where  $\Phi(x, y)$  is the function describing the basic shape of the gratings lines.

For the fundamental frequency,

$$\Phi(x, y) = 2n\pi$$

at the center of each bright line and is equal to an integer plus one-half times  $\pi$ ,

$$\Phi(x, y) = 2\pi(n + \frac{1}{2})$$

at the center of each dark line. The  $b$  coefficient determine the profile of the grating lines (i.e., square wave, triangular, sinusoidal, etc.) For a sinusoidal line profile,  $b_{1i}$  is only non-zero term.

When these two gratings are superimposed, the resulting intensity transmission function is given by the product

$$f_1(x, y)f_2(x, y) = a_1a_2 + a_1 \sum_{m=1}^{\infty} b_{2m} \text{Cos}[m\Phi_2(x, y)] + a_2 \sum_{n=1}^{\infty} b_{1n} \text{Cos}[n\Phi_1(x, y)] + \sum_{m=1}^{\infty} \sum_{n=1}^{\infty} b_{1n}b_{2m} \text{Cos}[n\Phi_1(x, y)] \text{Cos}[m\Phi_2(x, y)] \quad (2.4.3)$$

The first three terms of Eq.2.4.3 provide information that can be determined by looking at the two patterns separately; but the last term contains information about the relationships between the two grating functions.

It can be written as follows

$$\sum_{m=1}^{\infty} \sum_{n=1}^{\infty} b_{1n}b_{2m} \text{Cos}[n\Phi_1(x, y)] \text{Cos}[m\Phi_2(x, y)] = \frac{1}{2} b_{12}b_{21} \text{Cos}[\Phi_1(x, y) - \Phi_2(x, y)] + \frac{1}{2} \sum_{m=1}^{\infty} \sum_{n=1}^{\infty} \text{Cos}[n\Phi_1(x, y) - m\Phi_2(x, y)] + \frac{1}{2} \sum_{m=1}^{\infty} \sum_{n=1}^{\infty} b_{1n}b_{2m} \text{Cos}[n\Phi_1(x, y) + m\Phi_2(x, y)] \quad (2.4.4)$$

This expression shows that by superimposing the two gratings, the sum and difference between two gratings is obtained. The first term of Eq.2.4.4 represents the

difference between the fundamental pattern masking up the two gratings. it can be used to predict the moire' pattern in fig.2.2 Assuming that two grating are oriented with an angle  $2\alpha$  between them with the y-axis of coordinate system bisecting this angle as shown in fig 2.2.

Then the two grating functions  $\Phi_1(x, y)$  and  $\Phi_2(x, y)$  can be written as

$$\Phi_1(x, y) = \frac{2\pi}{\lambda_1}(x \cos \alpha + y \sin \alpha) \quad (2.4.5)$$

$$\phi_2(x, y) = \frac{2\pi}{\lambda_2}(x \cos \alpha - y \sin \alpha) \quad (2.4.6)$$

Where  $\lambda_1$  and  $\lambda_2$  are line spacings of the two gratings. Eq.2.4.5 and Eq.2.4.6 can be written as

$$\Phi_1(x, y) - \Phi_2(x, y) = \frac{2\pi}{\lambda_{beat}}x \cos(\alpha) + \frac{4\pi}{\lambda}y \sin \alpha \quad (2.4.7)$$

Where  $\bar{\lambda}$  is the average line spacing,  $\lambda_{beat}$  is the beat wave length between the two gratings given by

$$\lambda_{beat} = \frac{\lambda_1 \lambda_2}{\lambda_2 - \lambda_1} \quad (2.4.8)$$

$$\bar{\lambda} = \frac{\lambda_1 \lambda_2}{\lambda_2 + \lambda_1} \quad (2.4.9)$$

Note that this beat wavelength equation is the same as that obtained for two wavelength interferometry in Eq.2.4.4, the moire' or beat will be lines whose centers satisfy the equation

$$\Phi_1(x, y) - \Phi_2(x, y) = M2\pi \quad (2.4.10)$$

Three separate cases for moire' fringe can be considered [4, 11].

[1]. When  $\lambda_1 = \lambda_2 = \lambda$ , the first term of Eq.2.4.7 is zero, and the fringe center are given by

$$M\lambda = 2y \sin \alpha \quad (2.4.11)$$

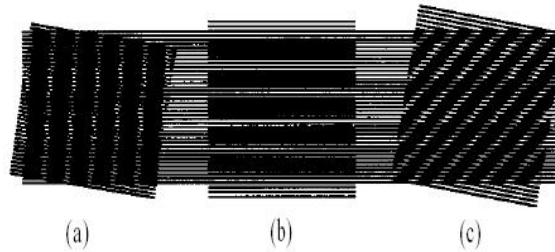


Figure 2.4: Moire pattern caused by two straight-line gratings with (a)the same pitch tilted with respect to one another, (b)different frequencies and no tilt,and (c) different frequencies tilted with respect to one another.

Where  $M$  is an integer corresponding to the fringe order. As we expected , Eq.2.4.10 is the equation of equi-spaced horizontal lines as seen in fig.2.3.

[2].The other simple case occurs when the gratings are parallel to each other with  $\alpha = 0$ .This makes the second term of Eq.2.4.7 The moire' will be line that satisfy

$$M\lambda_{beat} = X \quad (2.4.12)$$

These fringes are equally spaced, vertical lines parallel to the y-axis.

[3].For the more general case where two gratings have different line spacing and the angle between the grating is nonzero, the equation will now be

$$M\bar{\lambda} = \frac{\bar{\lambda}}{\lambda_{beat}}x \cos \alpha + 2y \sin \alpha \quad (2.4.13)$$

This is the equation of of straight lines whose spacing and orientation depends on the relative difference between two grating spacings and the angle between the gratings. fig. 2.3 shows moire'patterns for these three cases.

The orientation and spacing of the moire'fringes for the general case can be determined the geometry shown in fig 2.4 (Chiang,1983). The distance  $\overline{AB}$  can be written

in terms of the two grating spacings;

$$\overline{AB} = \frac{\lambda_1}{\sin(\theta - \alpha)} = \frac{\lambda_2}{\sin(\theta + \alpha)} \quad (2.4.14)$$

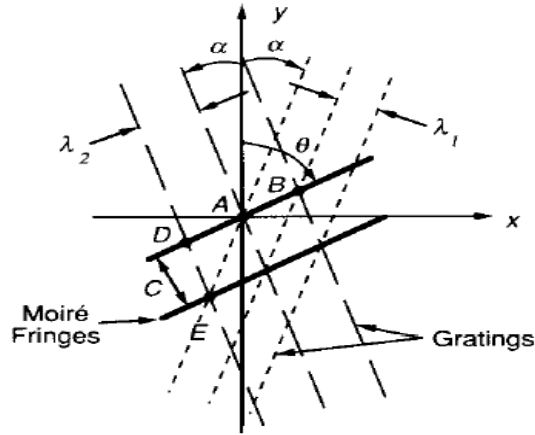


Figure 2.5: Geometry used to determine spacing and angle between two gratings of different frequencies

Where  $\theta$  is the angle the Moiré' fringes make with the y-axis. After rearranging the fringe orientation angle  $\theta$  is given by

$$\tan \theta = \tan \alpha \left( \frac{\lambda_1 + \lambda_2}{\lambda_2 - \lambda_1} \right) \quad (2.4.15)$$

When  $\alpha = 0$  and  $\lambda_1 \neq \lambda_2$ ,  $\theta = 0^\circ$  and when  $\lambda_1 = \lambda_2$  with  $\alpha \neq 0$   $\theta = 90^\circ$  are expected. The fringe spacing perpendicular to the fringe lines can be found by equating quantities for the distance  $\overline{DE}$

$$\overline{DE} = \frac{\lambda_1}{\sin 2\alpha} = \frac{C}{\sin(\theta + \alpha)} \quad (2.4.16)$$

Where C is the fringe spacing or contour interval. This can be rearranged to yield

$$C = \lambda_1 \left[ \frac{\sin(\alpha + \theta)}{\sin 2\alpha} \right] \quad (2.4.17)$$

By substituting for the fringe orientation  $\theta$ , the fringe spacing can be found in terms of the grating spacing and angle between the gratings;

$$C = \frac{\lambda_1 \lambda_2}{\sqrt{\lambda_2^2 \sin^2 2\alpha + (\lambda_2 \cos 2\alpha - \lambda_1)^2}} \quad (2.4.18)$$

In the limit that  $\alpha = 0$  and  $\lambda_1 \neq \lambda_2$ , the fringe space equals  $\lambda_{beat}$ , and in the limit that  $\lambda = \lambda_2 = \lambda_2$  and  $\alpha \neq 0$ , the fringe space equals  $\frac{\lambda}{2 \sin \alpha}$ . It is possible to determine  $\lambda_2$  and  $\alpha$  from the measured fringe spacing and orientation as long as  $\lambda_1$  is known (Chiang 1983).

## 2.4.2 Fringe Projection Techniques

A simple approach for contouring is to project interference fringes or grating onto an object and then view from another direction, as shown in fig 2.5.

Assuming a collimated illumination beam and viewing the fringe with a telocentric optical system, straight equally spaced fringes are incident on the object, producing equally spaced contour intervals. The departure of a viewed fringe from a straight line shows the departure of the surface from a plane reference surface. When the fringes are viewed at an angle  $\alpha$  relative to the projection direction, the spacing of lines perpendicular to the viewing direction will be

$$d = \frac{p}{\cos \alpha} \quad (2.4.19)$$

The contour interval  $C$  (the height between adjacent contour lines in the viewing direction) is determined by the line or fringe spacing projected onto the surface and the angle between the projection and viewing directions;

$$C = \frac{p}{\sin \alpha} = \frac{d}{\tan \alpha} \quad (2.4.20)$$

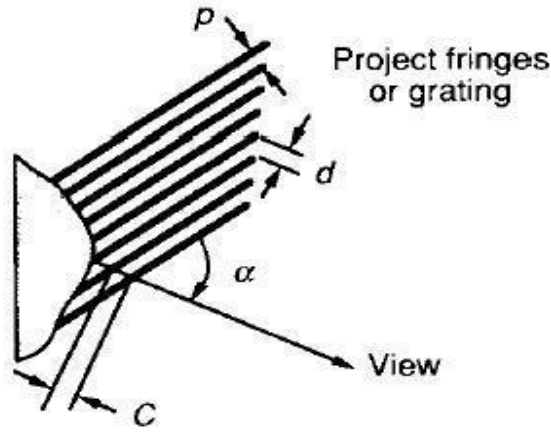


Figure 2.6: Projection of fringes or gratings onto an object and observing it at angle  $\alpha$ .  $P$  is gratings(pitch) and  $C$  the contour interval.

These contour lines are planes of equal height, and the sensitivity of the measurement is determined by  $\alpha$ . The larger the angle  $\alpha$ , the smaller contour interval. If the  $\alpha = 90^\circ$ , then the counter interval is equal top, and the sensitivity is maximum. The reference plane will be parallel to the direction of fringes and perpendicular to the viewing direction as shown in fig 2.6. Even though the maximum sensitivity can be obtained at  $90^\circ$ ,. When  $\alpha = 0$ , the counter interval is infinite and the measurement sensitivity is zero. For best results an angle no longer than the largest slope on the surface should be chosen.

When the interference fringes are projected onto surface rather than using grating, the fringe spacing  $P$  is determined by relation

$$P = \frac{\lambda}{2 \sin \Delta\theta} \quad (2.4.21)$$

where  $\lambda$  is the wave length of illumination and  $2\Delta\theta$  is the angle between the two interfering beams. Substituting the expression for  $P$  in to Eq.2.4.21, the contour

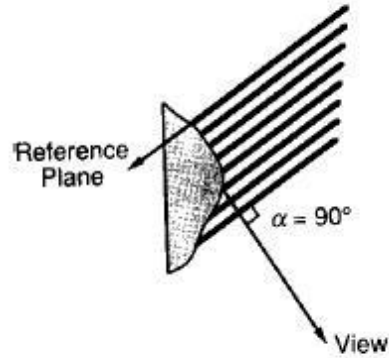


Figure 2.7: Maximum sensitivity for fringe projection at  $90^\circ$

interval becomes

$$C = \frac{\lambda}{2(\sin \Delta\theta) \sin \alpha} \quad (2.4.22)$$

Tilting one beam with respect to the other will change the counter interval; the larger the angle between the two beams the smaller the contour interval will be. If the source and the viewer are not at infinity, the fringe or grating are projected onto the object will not be composed of straight, equally spaced lines. The height between the contour planes will be a function of the distance from the source and viewer to the object [7, 12, 15].

### 2.4.3 Shadow Moire'

A simple method form of moire interferometry for counterimg objects uses a single grating placed in front of the object as shawon fig.2.8. The gratings in front of the object produces a shadow on the object that is viewed from different direction through the grating. A low frequency beat or moire pattern is seen. [20, 23]

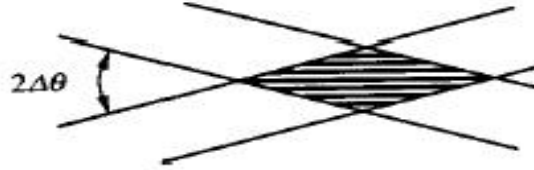


Figure 2.8: Fringe produced by two interfering beams

This pattern is due to the interference between the grating shadows on the object and the grating as viewed. Assuming that the illumination is collimated and that the object is viewed at infinity or through a telecentric optical system, the height  $z$  between the grating and the object point can be determined from geometry.

This height is given by

$$z = \frac{Np}{\tan \alpha + \tan \beta} \quad (2.4.23)$$

where:  $\alpha$  is the illumination angle,  $\beta$  is the viewing angle,  $p$  is the spacing of grating lines, and  $N$  is the number of grating lines between the points A and B (see in fig 2.8). The contour interval in a direction perpendicular to the grating will simply be given by

$$C = \frac{p}{\tan \alpha + \tan \beta} \quad (2.4.24)$$

Again, the distance between the moire' fringes in the beat pattern depends on the angle between the illumination and viewing directions. The larger the angle, the smaller

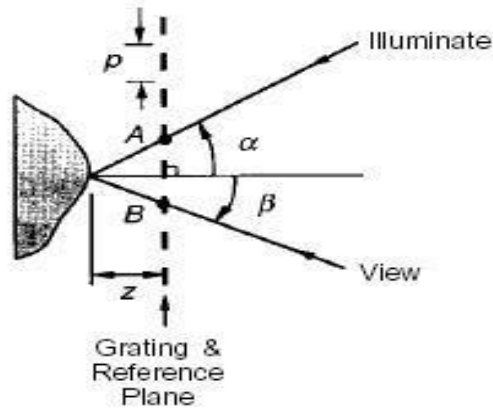


Figure 2.9: Geometry for shadow moiré' where illumination and viewing points are at infinity.

the contour interval, the reference plane will be parallel to the grating. Note that this reference plane is tilted with respect to the reference plane obtained when fringes are projected onto the subject. Essentially the shadow moiré' technique provides a way of removing the "tilt" term and repositioning the reference plane. Most of the time, it is difficult to illuminate an entire object with a collimated beam, Therefore, it is important to consider the case of finite illumination and viewing distances. However, for simplicity, only the case where the illumination and viewing positions are the same distance from the grating will be considered. The grating is assumed to be close enough to the object surface so that the direction effects are negligible. Figure 2.9 illustrates this phenomenon. [10]

The height between the object and the grating is given by

$$Z = \frac{Np}{\tan \beta' + \tan \alpha'} \quad (2.4.25)$$

Where  $\alpha'$  and  $\beta'$  are the illumination and viewing angles at the object surface. These

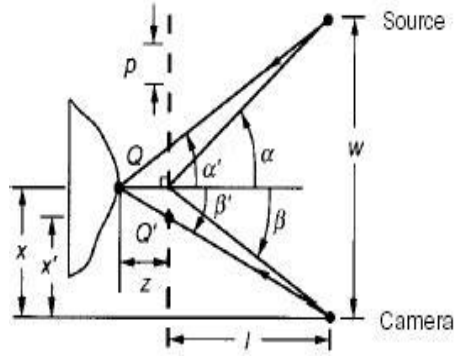


Figure 2.10: Shadow moiré when both illumination and viewing positions are at finite distances.

angles change for every point on the surface and are different from  $\alpha$  and  $\beta$ . Where  $\alpha$  and  $\beta$  are illumination and viewing angles at the reference surface. The surface height can be written as (Meadows et al. 1970; Takasaki1973; Chiang 1983)

$$Z = NC(z) = \frac{Np(l+z)}{w} = \frac{Npl}{w - Np} \quad (2.4.26)$$

This equation shows that the height is complex function depending on the position of the each object point. Thus the distance between contour interval is dependent on the height of the surface and the number of fringes between the grating and the object. Individual contour lines will no longer be planes of equal height. The expression for height can be simplified by considering the case where the distance to the source and viewer is large compared to the surface height variation,  $l \gg z$ . Then the surface height can be expressed as

$$Z = \frac{Npl}{w} = \frac{Np}{\tan \alpha + \tan \beta} \quad (2.4.27)$$

Even though the angles  $\alpha$  and  $\beta$  vary from point-to-point on the surface, the sum of their tangents remains equal to  $\frac{w}{l}$  for the object points as long as  $l \gg z$ . The contour interval will be constant. Because of the finite distances, there is also distortion due to the viewing perspective. A point on the surface  $Q$  will appear to be at the location  $Q'$ , when viewed through the grating. By similarity of triangles, the distances  $X$  and  $X'$  from the line perpendicular to the grating intersecting the camera location can be related using

$$\frac{X}{z+l} = \frac{X'}{l} \quad (2.4.28)$$

$\Rightarrow X = X'(1 + \frac{z}{l})$  Where  $X$  represent the actual coordinate in terms of the measured coordinates  $X'$ . Similarly the  $Y$ - coordinate can be corrected as

$$\frac{Y}{z+l} = \frac{Y'}{l} \quad (2.4.29)$$

$\Rightarrow Y = Y'(1 + \frac{z}{l})$ . This enables the measured surface to be mapped to the actual surface to correct the viewing perspective. These same factors can be applied to fringe projection.

#### 2.4.4 Projection Moire'

Moire' interferometry can also be applied to projecting interfering fringes or grating on to an object and then viewing through a second grating in front of the viewer.

The difference between the projection and shadow moire' is that two different gratings are used in the projection moire'. The orientation of the reference frame can be arbitrarily changed using different grating pitch to view the object. The contour

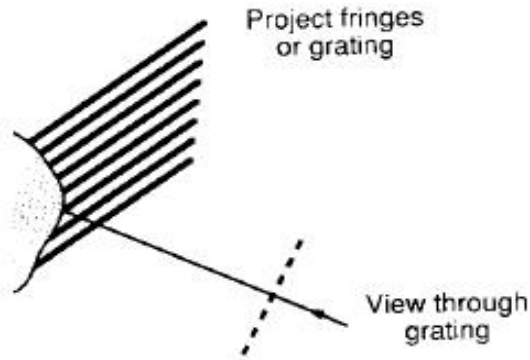


Figure 2.11: Projection Moire fringe

interval can be given by

$$C = \frac{d}{\tan \alpha + \tan \beta} \quad (2.4.30)$$

Where  $d$  is the period of grating in the plane. This makes the projection moire' the same as shadow moire' although projection moire' can be much more complicated than the shadow moire' [15, 16].

## 2.5 Moire Deflectometry

Laser moire' deflectometry applicable for , mini/micro-scale flow visualization is based on the moire' effect. The displacements of moire' fringes can be used to calculate deflection angle of laser beam , which is induced by the variation of refractive index of thermal flow fluid. The geometry scale less than 1mm is usually called

mini/micro-scale. when the conventional optical interferometry (eg. M-Z interferometry, Holographic interferometry, speckle interferometry etc.) is used, the needs of measurement sensitivity cannot be met because the phase variation produced by mini/micro-scale flow are vary small. in a general way 5-8 interferometry fringes in an interferogram are need to obtain accurate and reliable experimental data. However, when a light beam passes through the mini/micro-scale flow field, the number of interferometry fringe produced by phase variation of the flow field is often less than one. As a result it is very difficult to extract experimental data from the interferogram; sometimes it is impossible. However a light beam pass through mini/ micro-scale flow field, the moire' pattern contains more than five fringes can be captured [7, 11].

A He-Ne laser is used as a light source for visualization. The expanded and collimated light is formed using an expending lens  $L_1$  and collimation lens  $L_2$ . This parallel collimating beam passes through the flow field to measure and two gratings of amplitude type with the same pitch successively.  $L_3$  is microscopic image lens. because there is small angle between two gratings forming a series of moire' fringes with the diffracting order ( $0, \pm 1, \pm 2, \dots$ ) can be formed on image plane of  $L_3$  lens based on the moire' effect. The zero order moire' fringe is only imaged on the target of CCD by the means of an aperture D. the moire' fringe with information of mini/micro-scale flow are inputting to a microcomputer and are processed to extract the displacement of moire' fringes [16, 23].

Suppose that the pitch of both gratings  $G_1$  and  $G_2$  is  $P$  both and the angle between two gratings formed is  $\theta$ . The interval between two moire' fringes i.e spatial period  $T'$  of moire' fringes is

$$T' = \frac{P}{\theta} \quad (2.5.1)$$

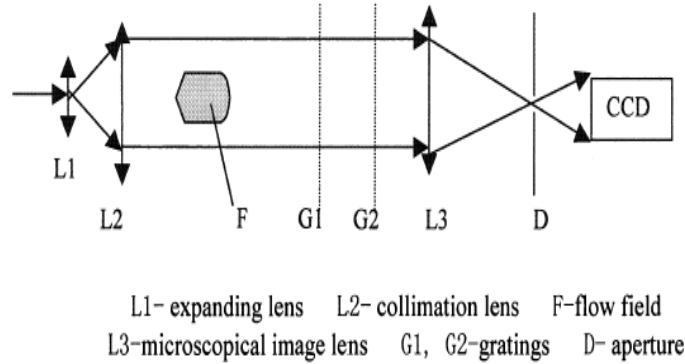


Figure 2.12: Experimental arrangement of laser moiré deflectometry.

Correspondingly, its basic spatial frequency  $f_0$  of the moiré' fringe is

$$f_0 = \frac{1}{T'} = \frac{\theta}{P} \quad (2.5.2)$$

If there is disturbance in flow fluid, the parallel detective light beam deflect after passing through the flow fluid. The deflection angle of light beam is  $\alpha$ , the relation between  $\alpha$  and displacement  $h$  of moiré' fringe is

$$\alpha = \frac{\theta h}{d} \quad (2.5.3)$$

Where  $d$ - the distance between two gratings. For a mini/micro-scale flow field, the deflection angle  $\alpha$  of the beam is very small, and the corresponding displacement  $h$  of the moiré' fringe is so small that is very difficult to measure directly.[11, 16] To improve the measurement accuracy for displacement of moiré' fringe, a method by phase measurement of moiré' fringe is proposed. The relation between phase  $\Phi$  and the displacement  $h$  of moiré' fringe is

$$\Phi = 2\pi f_0 h \quad (2.5.4)$$

Thus the deflective angle  $\alpha$  can be expressed as

$$\alpha = \frac{\theta h}{d}$$

but from Eq.2.5.4

$$h = \frac{\Phi}{2\pi f_0}$$

$$\alpha = \frac{\theta}{d} \left[ \frac{\Phi}{2\pi f_0} \right]$$

From Eq.2.5.2

$$p = \frac{\theta}{f_0}$$

$$\alpha = \frac{\Phi p}{2\pi d}$$

For a weak deflection, the relation between the deflection angle  $\alpha$  and the refractive index  $n$  is given by

$$\alpha = \frac{1}{n_e} \int_0^L \frac{\partial n}{\partial y} dz \quad (2.5.5)$$

Where  $n_e$ -environmental refractive index.  $L$ -is the length of test section. Thus, the phase-variation  $\Phi$  of moire' fringe can be written as the function of refractive index( $n$ )

$$\Phi = \frac{2\pi d}{pn_e} \int_0^L \frac{\partial n}{\partial y} dz \quad (2.5.6)$$

For a two dimensional flow field, the differential  $\frac{\partial n}{\partial y}$  of refractive index in y-direction can be obtained as

$$\frac{\partial n}{\partial y} = \frac{pn_e}{2\pi dL} \Phi \quad (2.5.7)$$

For an axi-symmetric flow field, the refractive index  $n_r$  can be written in following form by means of Abel transform

$$n_r - n_e = -\frac{n_e \theta}{\pi d} \int_r^\infty \frac{h(x, y)}{\sqrt{y^2 - r^2}} dy \quad (2.5.8)$$

$$n_r - n_e = -\frac{n_e f_0 p}{\pi d} \int_r^\infty \frac{h(x, y)}{\sqrt{y^2 - r^2}} dy \quad (2.5.9)$$

or

$$n_r - n_e = -\frac{n_e \theta}{\pi d} \int_r^\infty \frac{h(x, y)}{\sqrt{y^2 - r^2}} dy \quad (2.5.10)$$

$$n_r - n_e = -\frac{n_e p}{2\pi^2 d} \int_r^\infty \frac{\Phi(x, y)}{\sqrt{y^2 - r^2}} dy \quad (2.5.11)$$

If a fine grid or grating is illuminated from behind through usually, an identical grid or grating moire' fringes are produced on screen behind the second grid/ grating.[11] what is the imaged is the composite of pattern of near grid or grating and the shadow on it of the grid upstream , The nearer grating is undisturbed ,but the distortion of the light beam (such as its divergence or convergence) lead to distortion of the shadow component and corresponding distributions in the moire' fringe from their normally regular apprance. The distortion of the light beam could be produced by the presence of simple lens or more interestingly phase object whose optical power varies with position in it such a liquid with density or temperature gradients with in it.

Refractive index variations map onto these gratings. The refractive index variations then determine the shape of moiré fringe.

Moiré deflectometry is a wave front technique combining Talbot effect with moiré techniques for measuring and testing phase objects or refractive surfaces. Moiré deflectograms provided by the light deflection from tested phase objects or refractive surfaces can be used to calculate the deflection angle which represents the refractive index of the phase object or the height of the refractive surface. [4, 13, 16]

### 2.5.1 Phase Measuring Deflectometry

This is a new method of deflectometry applied to measure a specular free form surface within few seconds. The basic principle of the technique is to project the sinusoidal fringe patterns on a screen located remotely from the surface under test and to observe the fringe reflected via the surface. Any slope variation leads to a distortion pattern. Using a well known phase shifting algorithm, we can precisely measure these distortions and then calculate the surface normal in each pixel [4, 14].

Among the methods for extraction of phase from intensity distribution, the Fourier transform method of computer based fringe pattern analysis is more suitable for the mini or micro-scales flow visualization because a very small displacement of moiré fringes can be obtained. The mathematical model for extraction of phase from intensity distribution of moiré fringe is as follows. The intensity distribution  $I(x, y)$  of moiré fringe can be expressed as

$$I(x, y) = a(x, y) + b(x, y) \cos[2\pi f_0 X + \Phi(x, y)] \quad (2.5.12)$$

Where  $\Phi(x, y)$  is the phase that contains useful information and  $a(x, y)$  and  $b(x, y)$

are intensity factors which results from propagation of light beam.

In order to extract the phase Eq.2.5.12 transformed into the following form by

$$\Rightarrow e^{ix} = \cos x + i \sin x$$

$$I(x, y) = a(x, y) + C(x, y)\exp(i2\pi f_0 x) + \overline{C}(x, y)\exp(-i2\pi f_0 x) \quad (2.5.13)$$

Where

$$C(x, y) = \frac{1}{2}b(x, y)\exp(i\Phi(x, y)) \text{ and } \overline{C} = \frac{1}{2}b^*\exp(-i\Phi(x, y))$$

By using one-dimensional Fourier transformer for x-coordinate Eq.2.5.12 transfer

$$I(x, y) = A(f, y) + C(f - f_0, y) + \overline{C}(f + f_0, y) \quad (2.5.14)$$

Where f is the spital frequency in x-coordinate Eq.2.5.13 expresses function of frequency distribution corresponding to Eq.2.5.12. The capital letters are the coefficient of Fourier transform.

In order to extract the phase factor from the spital frequency distribution, a band-pass filter is used. As a result, the term  $C(f - f_0, y)$  is kept only. The expression of Fourier inverse transformation for the term  $C(f - f_0, y)$  can be written as

$$C'(x, y) = \frac{1}{2}b(x, y)\exp i[\Phi(x, y) + 2\pi f_0 x] \quad (2.5.15)$$

Using identical transformation Eq.2.5.15 becomes

$$C'(x, y) = \frac{1}{2}b(x, y)\cos[\Phi(x, y) + 2\pi f_0 x] + i \sin[\Phi(x, y) + 2\pi f_0 x] \quad (2.5.16)$$

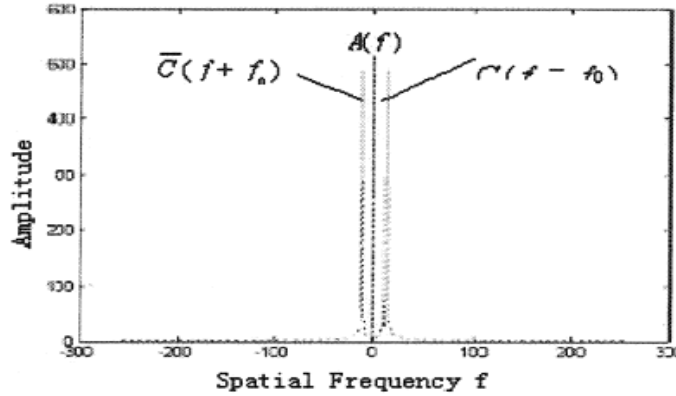


Figure 2.13: Spatial frequency distribution of moire' fringes

Thus the phase factor  $\Phi(x, y)$  can be extracted from Eq.2.5.16

$$\Phi(x, y) = \arctan \frac{\text{Im}(c')}{\text{Re}(c')} - 2\pi f_0 x \quad (2.5.17)$$

Where  $\text{Im}(c')$  and  $\text{Re}(c')$  imaginary and real component of complex  $c'$  respectively. Because of parodic property of intensity function for moire' fringes, only main phase value can be obtained from moire' fringe pattern by Fourier transform [11, 14].

## 2.6 Diffusion Coefficient and Moire' Fringe Shift.

The Moire Deflectometry experimental set-up Used to measure the diffusion coefficient of transparent solution. The deflected laser beam due to changes in refractive index in the diffusion cell yields the shifted self-image on gratings and resultant Moire' fringes show a deviation [20, 23].

For an isothermal mixture, with out generation and recombination, the physical

problem associated with the experiment described above can be formulated mathematically. A diffusion column of constant cross-section, extended in the x-direction, and the concentration varying with the position coordinate x only. Thus, the diffusion process can be formulated in terms of one-dimensional problem.

The free diffusion process is governed by Fick's second law, and for one dimensional diffusion along x-axis it is given by

$$\frac{\partial C(x, t)}{\partial t} = D \frac{\partial^2 C(x, t)}{\partial x^2} \quad (2.6.1)$$

Where  $C(x, t)$  is the concentration at position x at time t, D is the diffusion coefficient, assumed to be independent of concentration, and x is the direction of diffusion. If there is the net external force, F (e.g. gravitational force), acting in the x-direction up on the dissolved molecules and if  $\mu$  be the mobility of the molecules under consideration (i.e. the steady velocity, acquired under the action of unit force) the steady velocity of these molecules would be  $\mu.F$  and the resulting flux of matter would be  $\mu.FC(x, t)$ .

Consequently the rate of concentration changes would then become

$$\frac{\partial C}{\partial t} = D \frac{\partial^2 C(x, t)}{\partial x^2} - \mu F \frac{\partial C(x, t)}{\partial x} \quad (2.6.2)$$

It is even possible to reduce the problem of eq.2.6.2 to that of ordinary diffusion eq.2.6.1 by the means of following transformation

$$C(x, t) = C^*(x, t) \exp\left[-\frac{\mu F x}{2D} - \frac{\mu^2 F^2 t}{4D}\right] \quad (2.6.3)$$

Where  $C^*$  is the function that satisfies eq.2.6.1 If the steady velocity of the dissolved molecules( $\mu F$ ) is very slow the current due to the external forces can be neglected and eq.2.6.2 reduce to equ.2.6.1. The solution of equ.2.6.1, for two binary liquid mixtures initially( $t=0$ ) separated at ( $x=0$ ) with concentration  $C_o$  and  $C_1$  is an error function given by

$$C(x, t) = \frac{C_0 - C_1}{2} + \frac{C_0 - C_1}{2} \operatorname{erf}\left[\frac{X}{2\sqrt{Dt}}\right] \quad (2.6.4)$$

Where the error function is defined as

$$\operatorname{erf}(x) = \frac{2}{\sqrt{\pi}} \int_0^x e^{-t^2} dt \quad (2.6.5)$$

On the other hand, if we consider the solution of eq.2.6.1 in eq.2.6.5  $x$  is replaced by  $x - \mu gt$ . In this case the influence of gravity causes a change in the central diffusion location, that is another layer as the second center of diffusion will formed [6, 11].

In a transparent mixture, a change in the concentration produces a change of refractive index, which for the small concentration gradient can be considered a linear function between refractive index and concentration.

The refractive index gradient is given by

$$\frac{\partial n(x, t)}{\partial x} = \frac{n_0 - n_1}{2\sqrt{\pi Dt}} \exp\left[-\frac{X^2}{4Dt}\right] \quad (2.6.6)$$

Where  $n(x, t)$  is the local index at time  $t$  in the diffusion cell,  $n_0$  the refractive index of high concentration solution and  $n_1$  that of low concentration solution. If the refractive index changes the rays contributing to the formation of the Moire' fringes pattern will be deflected locally according to refractive index distribution, accordingly the Moire' fringes will also change.

The incident parallel laser beam passing through the diffusion cell, bends by angle  $\Psi(x, t)$  depending on the distribution of the refractive index on the cell. Because the refractive index (concentration) depends on position (X) and time (t), accordingly, the deflection angle also would be position and time dependent. Due to the deflection of the collimated beam, imaging on the deflectionometry system, the Fourier image of the first grating shifts on the second grating[25].

For small bending of light rays, the amount of Fourier image shift would be  $\Psi(x, t)Z_t$ . The displacement of the Fourier image of the first grating on the second one, the Moire' fringe to shift with respect to the original locations. The amount of fringe shift  $\Delta\xi(x, t)$  is given by

$$\Delta\xi(x, t) = \frac{Z(t)}{\theta}\Psi(x, t) \quad (2.6.7)$$

Where  $\theta$  a small tilt angle between the intersection of the grating lines and  $Z_t$  is the  $t^{th}$  talbot distance between gratings. The desired information from diffusion process is contained in  $\Psi(x, t)$ . On the other hand, the relation between the integrated deflection angle and the refractive index  $n(x, t)$  is

$$\Delta\Psi(x, t) = \frac{1}{n_a} \int_0^L \left[ \frac{\partial n(x, y, z, t)}{\partial x} \right]_{y=const} dz \quad (2.6.8)$$

Where  $n_a$  is the ambient refractive index along the x-axis diffusion, the direction and L represents the thickness of diffusion cell measured along the propagation axis (z-axis). The diffusion process is assumed to occur only along the x-direction, so the index of refraction along the Z-direction remain constant and the Equ.2.6.8 becomes

$$\Psi(x, t) = \frac{d}{n_a} \frac{\partial n(x, t)}{\partial x} \quad (2.6.9)$$

Taking into account *Equ.2.6.7* and *Equ.2.6.8* can be written as

$$\Delta\xi(x, t) = \frac{Z_t}{n_a\theta} \frac{\partial n(x, t)}{\partial x} \quad (2.6.10)$$

*Equ.(65)* shows the Moire' Fringe deformation is proportional to the refractive index gradient introduced by the diffusion process[11, 25].

By replacing *Equ.2.6.6* and *Equ.2.6.10* the corresponding local shift of Moire'Fringes results

$$\Delta\xi(x, t) = \frac{Z_t d}{n_a\theta} \frac{n_0 - n_1}{2\sqrt{\pi Dt}} \exp\left[\frac{-x^2}{4Dt}\right] \quad (2.6.11)$$

Where for simplicity,  $\Delta_0$  defined as

$$\Delta_0 = \frac{Z_t d(n_0 - n_1)}{n_a 2\theta\sqrt{\pi D}} \quad (2.6.12)$$

$$\Delta\xi(x, t) = \frac{\Delta_0}{\sqrt{t}} \exp\left[\frac{-x^2}{4Dt}\right] \quad (2.6.13)$$

The diffusion coefficient can be obtained from a single Moire' pattern recorded at time instant  $t_0$ .

For two distance  $x_1$  and  $x_2$ , then ( $x_2 > x_1$ ) along the diffusion cell , the local shift of Moire' fringes would be:

$$\Delta_1 = \frac{Z_t L}{\theta} \frac{n_o - n_1}{n_a 2\sqrt{\pi Dt_o}} \exp\left[\frac{-x_1^2}{4Dt_o}\right] \quad (2.6.14)$$

$$\Delta_2 = \frac{Z_t L}{\theta} \frac{n_o - n_1}{n_a 2\sqrt{\pi Dt_o}} \exp\left[\frac{-x_2^2}{4Dt_o}\right] \quad (2.6.15)$$

The ratio of two local shift is

$$\eta = \frac{\Delta_1}{\Delta_2} = \exp\left[\frac{-x_1^2 - x_2^2}{4Dt_0}\right] \quad (2.6.16)$$

Then the diffusion coefficient can be defined as

$$D = \frac{x_2^2 - x_1^2}{4t_0 \ln \eta} \quad (2.6.17)$$

# Chapter 3

## Experimental Technique

### 3.1 Materials and Methods of the Experiment

In laser moire'deferectometry experimental set up used to measure the diffusion coefficient of sugar solution in pure water at room temperature. In this experiment the moire fringes are observed on screen attached to concave lens 10cm focal length. a diffusion cell of rectangular cross section with the plane glass of  $3 \times 3 \times 14\text{cm}^3$  the longer dimension gives the direction of diffusion placed in front of gratings

### 3.2 Experimental Methods and Procedures

Helium-Neon laser source with wave length of 632.8nm that can deliver a power of 1mw was sent through a convex lens of focal length 10cm, and convex lens with focal length 5cm, that expanded parallel beams scans the whole column of grating passing through the solution. A solution of higher density and the same volume was into the diffusion cell by capillary tube from bottom of the tube. The diverging lens of focal

length of 10cm ,was used to form fringe on the screen.

A digital camera that has a resolving power of  $2848 \times 2136$  pixies was used to take the image from semitransparent screen.In order to achieve constant results, the camera was also mounted on stand and had been kept fixed until the experiment was over.



Figure 3.1: Experimental set up

### 3.3 Procedure

The half diffusion cell first filled with light solution (low concentration) and followed by the heavier solution (high concentration) of equal volume introduced below by 10ml siring.After the cell filed the diffusion cell filled the diffusion process starts.

The following apparatus are also used in doing the experiment. He-Ne laser source with power 1mw,wave length 632.8nm, convex lens of focal length 5cm,convex lens focal length 10cm,adjustable slit,Diffusion cell  $3cm \times 14cm$ ,Diffraction grating

with 100 lines/mm, balance, concave lens of focal length 10cm, beakers, semitransparent screen, and digital camera.

### **3.4 Materials Used**

I was prepared different concentration of sugar by mass-volume ratio. For example to prepare 5 percent sugar solution, I was dissolve 5 gram of sugar in 95 gram of distilled water. By similar procedure I was prepared different percent of sugar solution. The materials used for this experiment were: 2.5, 5, 7.5, 10, 12.5, 15, 17.5, and 20 percents of sugar solution.

# Chapter 4

## Results, Analysis and Discussion

### 4.1 Determination of diffusion coefficient of Sugar Solution in different concentration

The diffusion coefficient of a solute in solvent depend on temperature, concentration, size of particle and the time taken for diffusion. The concentration of solution in this experiment is also the function of position and time. The following figures and analysis were made for various concentration.

#### 4.1.1 Sugar Solution Concentration 2.5 percent

The following photograph were taken by a digital camera at different time fig (a), (b),(c) show the shift in fringes after 18hrs,24hrs,30hrs respectively. the relative position of adjacent fringe f4rom vertical axis was measured.

Table 1. Shifts in fringe 2.5 percent sugar solution after 18 hrs, 24 hrs and 30 hrs,

respectively

Time	$t_0=18$ hrs	$t_1=24$ hrs	$t_2=30$ hrs
Shift	$X_0=0.10$ cm	$X_1=0.12$ cm	$X_2=0.16$ cm

The local shift of fringes became

$$\Delta_2 = X_2 - X_1 = 0.04cm$$

$$\Delta_1 = X_1 - X_0 = 0.02cm$$

The ratio of local shift is given by

$$\eta = \frac{\Delta_1}{\Delta_2} = 0.5$$

The diffusion coefficient is calculated by using the equation

$$D = \frac{X_2^2 - X_0^2}{4t_0 \ln \eta} = (0.008) \times 10^{-5} \frac{cm^2}{s}$$

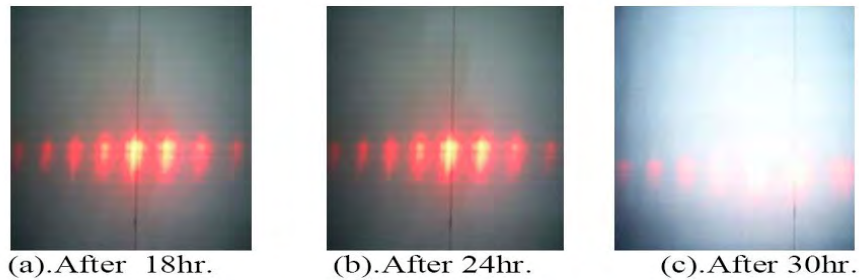


Figure 4.1: Fringe Shift in 2.5 percent sugar solution

#### 4.1.2 Sugar solution concentration 5 percent

The same procedure was repeated for 5 percent under the same condition of the experiment. The position of fringes were (a),(b), (c), noted after 16hrs,22hrs,28hrs.

Table 2. Shifts in fringe 5 percent sugar solution after 16 hrs, 22 hrs and 28 hrs, respectively

Time	$t_0=16$ hrs	$t_1=22$ hrs	$t_2=28$ hrs
Shift	$X_0=0.16$ cm	$X_2=0.18$ cm	$X_2=0.21$ cm

The local shift of fringes became

$$\Delta_2 = X_2 - X_1 = 0.02\text{cm}$$

$$\Delta_1 = X_1 - X_0 = 0.03\text{cm}$$

The ratio of local shift is given by

$$\eta = \frac{\Delta_1}{\Delta_2} = 0.6$$

The diffusion coefficient

$$D = \frac{X_2^2 - X_0^2}{4t_0 \ln \eta} = (0.010) \times 10^{-5} \frac{\text{cm}^2}{\text{s}}$$

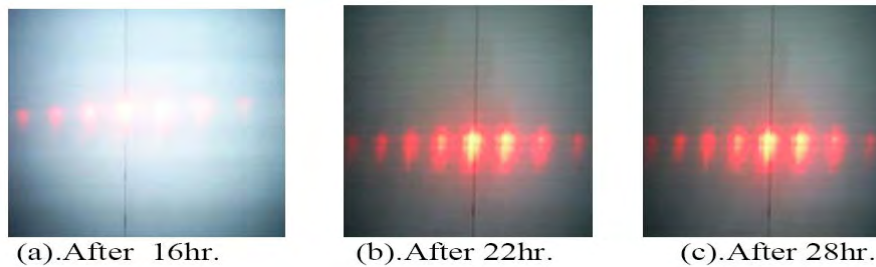


Figure 4.2: Fringe Shift in 5 percent sugar solution

### 4.1.3 Sugar Solution Concentration 7.5 percent

The same procedure was repeated for 7.5 percent under the same condition of the experiment. The position of fringes were (a),(b), (c), noted after 24hrs,30hrs,48hrs.

Table 3. Shifts in fringe 7.5 percent sugar solution after 24 hrs, 30 hrs and 48 hrs, respectively

Time	$t_0=24$ hrs	$t_1=30$ hrs	$t_2=48$ hrs
Shift	$X_0=0.15$ cm	$X_1=0.17$ cm	$X_2=0.20$ cm

The local shift of fringes became

$$\Delta_1 = X_1 - X_0 = 0.02\text{cm}$$

$$\Delta_2 = X_2 - X_1 = 0.03\text{cm}$$

The ratio of two local shift

$$\eta = \frac{\Delta_1}{\Delta_2} = 0.6$$

The diffusion Coefficient

$$D = \frac{X_2^2 - X_0^2}{4t_0 \ln \eta} = (0.015) \times 10^{-5} \frac{\text{cm}^2}{\text{s}}$$

### 4.1.4 Sugar Solution Concentration 10 percent

The same procedure was repeated for 10 percent under the same condition of the experiment. The position of fringes were (a),(b), (c), noted after 24hrs,30hrs,48hrs.

Table 4. Shifts in fringe 10 percent sugar solution after 24 hrs, 30 hrs and 48 hrs, respectively

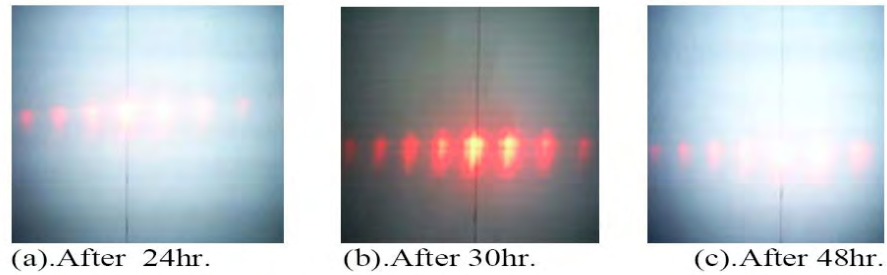


Figure 4.3: Fringe Shift in 7.5 percent sugar solution

Time	$t_0=24$ hrs	$t_1=30$ hrs	$t_2=48$ hrs
Shift	$X_0=0.40$ cm	$X_1=0.70$ cm	$X_2=1.50$ cm

The local Shift of fringe became

$$\Delta_1 = X_1 - X_0 = 0.3cm$$

$$\Delta_2 = X_2 - X_1 = 0.8cm$$

The ratio of two local shift

$$\eta = \frac{\Delta_1}{\Delta_2} = 0.375cm$$

The diffusion coefficient calculated using the equation

$$D = \frac{X_2^2 - X_0^2}{4t_0 \ln \eta} = 0.67 \times 10^{-5} \frac{cm^2}{s}$$

The value obtain by diffusion coefficient then became

$$(0.67 \pm 0.21) \times 10^{-5} \frac{cm^2}{s}$$

. The value obtained for 10percent sugar solution in my work was comparable to that one found by digital holography interferometry,which is in reasonable agreement with published data was[7, 23]

$$(0.66 \times 10^{-5} \frac{cm^2}{s})$$

,also to similar experiment by moire'pattern are projected on computerized CCD camera by a lens placed at the back of the second grating

$$(0.65 \times 10^{-5} \frac{cm^2}{s})$$

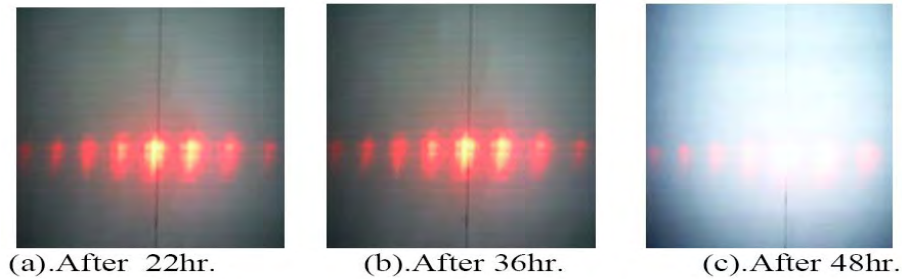


Figure 4.4: Fringe Shift in 10 percent sugar solution

#### 4.1.5 Sugar Solution Concentration 12.5 percent

The same procedure was repetend for 12.5 percent under the same condition of the experiment. The position of fringes were (a),(b), (c),noted after 22hrs,36hrs,48hrs.

Table 5. Shifts in fringe 12.5percent sugar solution after 22 hrs, 36 hrs and 48 hrs, respectively

Time	$t_0=22$ hrs	$t_1=36$ hrs	$t_2=48$ hrs
Shift	$X_0=0.70$ cm	$X_1=0.93$ cm	$X_2=1.65$ cm

The local Shift of fringe became

$$\Delta_1 = X_1 - X_0 = 0.11cm$$

$$\Delta_2 = X_2 - X_1 = 0.89cm$$

The ratio of two local shift

$$\eta = \frac{\Delta_1}{\Delta_2} = 0.12cm$$

The diffusion coefficient calculated using the equation

$$D = \frac{X_2^2 - X_0^2}{4t_0 \ln \eta} = (0.86) \times 10^{-5} \frac{cm^2}{s}$$

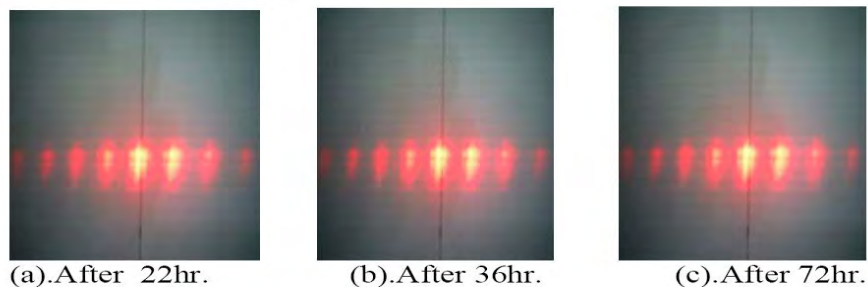


Figure 4.5: Fringe Shift in 12.5 percent sugar solution

#### 4.1.6 Sugar Solution Concentration 15 percent

The same procedure was repeated for 15 percent under the same condition of the experiment. The position of fringes were (a),(b), (c), noted after 22hrs,36hrs,72hrs.

Table 6. Shifts in fringe 15 sugar solution after 22 hrs, 36 hrs and 48 hrs, respectively

Time	$t_0=22$ hrs	$t_1=36$ hrs	$t_2=72$ hrs
Shift	$X_0=0.7$ cm	$X_1=1.23$ cm	$X_2=1.87$ cm

The local Shift of fringe became

$$\Delta_1 = X_1 - X_0 = 0.53\text{cm}$$

$$\Delta_2 = X_2 - X_1 = 0.64\text{cm}$$

The ratio of two local shift

$$\eta = \frac{\Delta_1}{\Delta_2} = 0.86\text{cm}$$

The diffusion coefficient calculated using the equation

$$D = \frac{X_2^2 - X_0^2}{4t_0 \ln \eta} = (0.91) \times 10^{-5} \frac{\text{cm}^2}{\text{s}}$$

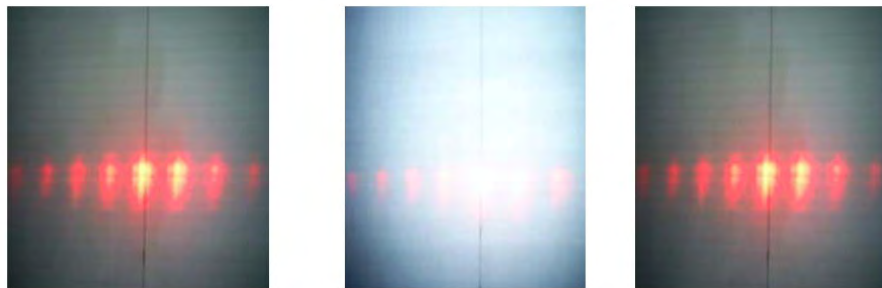


Figure 4.6: Fringe Shift in 15 percent sugar solution

### 4.1.7 Sugar Solution Concentration 17.5 percent

Similar procedure yields the following data for concentration,17.5percent under the same condition of the experiment. The position of fringes were (a).after 24hrs(b).after 48hrs (c).after72hrs

Table 7. Shifts in fringe 17.5percent sugar solution after 24 hrs, 48 hrs and 3 days, respectively

Time	$t_0=24$ hrs	$t_1=48$ hrs	$t_2=72$ hrs
Shift	$X_0=0.75$ cm	$X_1=1.25$ cm	$X_2=1.93$ cm

The local Shift of fringe became

$$\Delta_1 = X_1 - X_0 = 0.51cm$$

$$\Delta_2 = X_2 - X_1 = 0.68cm$$

The ratio of two local shift

$$\eta = \frac{\Delta_1}{\Delta_2} = 0.71cm$$

The diffusion coefficient calculated using the equation

$$D = \frac{X_2^2 - X_0^2}{4t_0 \ln \eta} = 3.3 \times 10^{-5} \frac{cm^2}{s}$$

### 4.1.8 Sugar Solution Concentration 20 percent

Similar procedure yields the following data for concentration,20percent under the same condition of the experiment. The position of fringes were (a).after 22hrs(b).after 72hrs (c).after6days

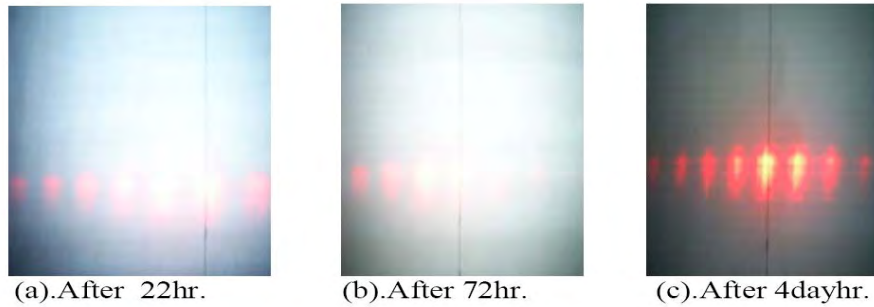


Figure 4.7: Fringe Shift in 17.5 percent sugar solution

Table 8. Shifts in fringe 20percent sugar solution after 22 hrs, 72 hrs and 6 days, respectively

Time	$t_0=22\text{hrs}$	$t_1=72\text{hrs}$	$t_2=6\text{days}$
Shift	$X_0=0.75\text{cm}$	$X_1=1.25\text{cm}$	$X_2=1.98\text{cm}$

The local Shift of fringe became

$$\Delta_1 = X_1 - X_0 = 0.51\text{cm}$$

$$\Delta_2 = X_2 - X_1 = 0.73\text{cm}$$

The ratio of two local shift

$$\eta = \frac{\Delta_1}{\Delta_2} = 0.71\text{cm}$$

The diffusion coefficient calculated using the equation

$$D = \frac{X_2^2 - X_0^2}{4t_0 \ln \eta} = 3.31 \times 10^{-5} \frac{\text{cm}^2}{\text{s}}$$

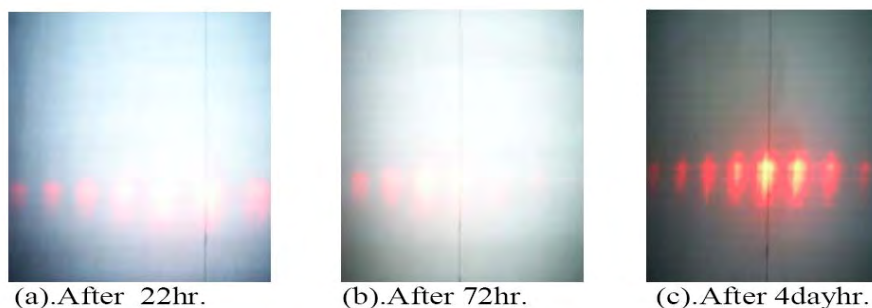


Figure 4.8: Fringe Shift in 20 percent sugar solution

#### 4.1.9 Discussion

Moiré deflectometry provides data about changes of concentration/ refractive index between two different concentrations. Moiré pattern shows in the beginning of experiment when the laser beam scans a uniform area. As the heavier solution in the lower part of the diffusion cell pushes the lighter solution to the top of the cell, the moiré fringes, due to both the solutions, can be seen simultaneously. The refractive indices at various planes along the diffusion cell are different and the liquid passing through the cell will have different optical paths.

In a transparent mixture, change in concentration for a multi-component liquid mixture, results a change in index of refraction. A parallel laser beam passing through such a medium of varying index of refraction, is locally deflected even if it passes perpendicularly to the gradient of index of refraction in the diffusion direction. The deflection angle is direct mapping of the refractive index gradient of the medium.

In the Moiré refractometry technique, the monitored area is restricted by the laser beam and grating size. The wide expand of laser beam and larger grating size it is possible to monitor large areas of diffusion cell.

In 10 percent sugar solution the value of by diffusion coefficient became

$$(0.67 \pm 0.22) \times 10^{-5} \frac{cm^2}{s}$$

. This value is comparable to that one found by digital holography which was

$$(0.65 \times 10^{-5} \frac{cm^2}{s})$$

,also to similar experiment by CCD was

$$(0.66 \pm 0.05) \times 10^{-5} \frac{cm^2}{s}$$

,and also another experiment, one found by digital camera

$$(0.68 \pm 0.18) \times 10^{-5} \frac{cm^2}{s}$$

I repeated experiment with higher sugar concentration 17.5 percent and 20 percent. In the case of 17.5 percent after 2 days after the beginning of diffusion there is no bending in moire fringes. It is observed that after 4 days of diffusion, a dens layer formed above the initial boundary of the two solutions. Similarly in the case of 20 percent after 4 days after the beginning of diffusion there is no bending in moire fringes. It was after 6 days, a dens layer formed above initial boundary of the two solution.

The existence of this layer due to the effect of gravitation on diffusant sugar molecules, where the up ward motion of molecules balances with the down ward drift velocity due to gravity and the molecules become stationary.

In the case of influence of gravity causes change in the central diffusion location, that is another layer as the second center of diffusion will form. This effect so called baro-diffusion effect.

#### 4.1.10 Diffusion Vs concentration graph

the incident laser beam passes through the diffusion cell, it bend by small angle, depending on the distribution of refractive index on the cell. Because the refractive index and concentration depends on time and position ,accordingly deflection angle also time and position dependent. In transparent solution change in concentration produce change of index of refraction. Due to deflection of collimated beam on the refractometries system the displacement of image of first grating cause fringe shift from original direction

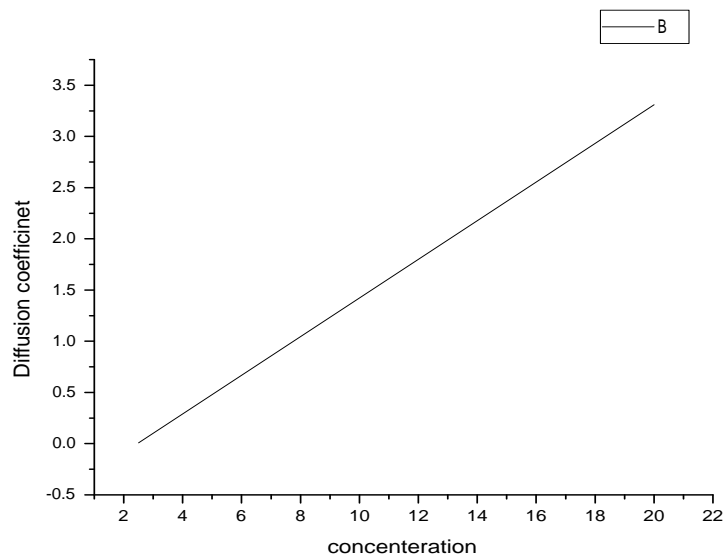


Figure 4.9: Diffusion Coefficient Vs Concentration

This implies that in transparent solution, the diffusion coefficient and small concentration gradient can be a linear function between refractive index and concentration.

# Chapter 5

## Conclusion

### 5.1 Conclusion

Moire deflectometry is a power tool for determining diffusion coefficient of transparent liquid solution and it includes direct mapping of ray deflection due to the change of refractive index of diffusion medium. This leads to local perturbation of a collimated laser incident beam which is mapped by more fringes patterns. The results show that ray deflection increase with the increase in concentration and at increase in concentration will increase the index of refraction of the solution which in turn increase in the angle of refraction of the emergent ray.

Also the results show that the Moire' fringes shift according to the refractive index distribution inside the diffusion medium describe the relation between the change in the moire fringes and the deflection angle of the laser beam that passes through the diffusion cell.

In higher sugar concentration example 17.5 percent and 20percent, the formation of a dens layer above the initial boundary layer, which may be due to so-called baro

diffusion effect, where the upward current of diffusion is balanced with the downward drift current by gravity.

# Bibliography

- [1] Arun Anand\*,K.Vanic Chhaniwal and CS Narayana Murthy Diffusivity Study Of Transparent Liquid sluttion by imaging Beam Deflection.
- [2] Bocher N and Pipman J 1976 A Simple method of determining Diffusion Constents By Holographic Interferometry J.Phys.D:Appl.Phys.9 1825-30.
- [3] Born M and Wolf E 1986 Principles of Optices 6<sup>th</sup> edn.(Oxford:Perogamon)
- [4] Crank E.J.1975 *The Mathematices of Diffusion* (Oxford:Oxford University Press).
- [5] Guild J.The Interference Systems of Crossed Diffraction Gratings, Clarendon Press,Oxford,1956
- [6] Howard .M.Smith *Principle of Holography*, Printed in the United state of America (1969)
- [7] Jamshidi-Ghaleh.K,Taghi Tavasoly.M and Mansour.N Published 30 June 2004 PhysD/37/1993
- [8] J Hiddik,Physics of Electerolytes ACADIMIC PRESS INCE.LONDON(1972)
- [9] Jost.W 1970 Diffusion in Solids,Liquids,Gas (New York: Academic)

- [10] Kafri O and Glatt I 1986 Moire' Defeectometry:a ray defelection testing  
Opt.Eng 24 944-60
- [11] Krasinki M.J 1996 Evolution Of Diffusion fildes around KDP Crystal graowing  
in gel crystal. *Res.Technol* 34 647-53.
- [12] Kung H,L.Bhatnager A and Muiller DAB 2001 Opt.Lett 26 1645
- [13] L.Mertz,Real-Time Fringe Pattern Analysis Appl Opt Vol 22 No 10 P 1535 (1983)
- [14] MacGovem,A.J,Projected Fringes and Holography,Appl.Opt11 (12),2972-  
74(1972)
- [15] Mathur B.K Principle of Optices,ACADIMIC PRESS INCE.NEW YORK  
(1966)¶.180-82
- [16] Mayinger F(ed) 1994 *Optical Measurments* (Berlin:Springer).
- [17] Moire' and Fringe Projection Techinques Optical shope Testing,second Edition  
,Edited by Danial Malacra. ISBN 0-471-5223-5(1992),John Wiley and Sons,inc.
- [18] Moor,D.T.and B.E.Truxax,Phase-Locked Moire' Fringe Anlysis for Automated  
Counterling of Diffuse Surfaces Appl.Opt.18(1),91-96(1979)
- [19] N.J Giordon,H.Prentice Computitional Physics (1997).
- [20] Steven L.Jacques,Scott A.Prahl,Fikes Lawes of Diffusion;ECE532 Biomedical  
Optices(1998).
- [21] Thecaries,P.S,Moire Fringes In Strine Analysis,Pregamon Press, Oxford (1969)

- [22] W.W.Macy Jr."Two-Dimensional Fringe-Pattern Analysis",Appl Opt.Vol 22 p 3898 (1983)
- [23] Yaozu.S,Xiangchun.Z,Honglinin.Z Departement of Enginner Mechanics,Laser Moire' Defelectomrtery Applicabel for Mini/Micro-Scale Flow Visulaization.
- [24] Zhixiong G,Maruyama S and Komiya A 1999 Rapide yet accurate Measurment of mass diffusion Coefficinnet by Phase shifting interferometer J.Phy.D:Appl.Phys.32 995-9.
- [25] Zydowska J and Janswska B 1983 Holographic measurment of DiffusionJ.Phys.D:Appl.Phy.15 1385-93